

Article

STATISTICAL EQUILIBRIUM OF CIRCULATING FLUIDS

Alexander Migdal ^{1,t,‡} ¹ SPD, Abu Dhabi Investment Authority, 211 Corniche Street, Abu Dhabi 3600, Abu Dhabi, United Arab Emirates; alexander.migdal@adia.ae² Department of Physics, New York University Abu Dhabi, Saadiyat Island, Abu Dhabi, PO Box 129188, Abu Dhabi, United Arab Emirates; am10485@nyu.edu

* Correspondence: sasha.migdal@gmail.com

Abstract: We develop a new theory of circulation statistics in strong turbulence, treated as a fixed point of a Hopf equation. Strong turbulence is the limit of vanishing viscosity in the Navier-Stokes equation. We use spherical Clebsch variables to parametrize vorticity in the stationary singular Euler flow with a phase gap in the angular Clebsch variable across a discontinuity surface bounded by a stationary loop C in space. We find a circular vortex with a singular core on this loop, regularized as a limit of the Burgers vortex. We find anomalous contributions to the Euler Hamiltonian and to the energy flow, staying finite in the limit of vanishing viscosity. Normalization constant in the spherical Clebsch variables is determined from the energy balance between incoming flow and anomalous dissipation. As a result, we compute the PDF of velocity circulation Γ , which decays exponentially with pre-exponential factor $1/\sqrt{\Gamma}$ in perfect match with numerical simulations of conventional forced Navier-Stokes equations on periodic lattice $16K^3$.

Keywords: Turbulence; Euler; Clebsch; Statistics, Winding, Intermittency

0. Introduction. Path to the summit

The unsolved problem of classical turbulence has challenged us for centuries, like a shining Himalaya peak.

Burgers, Onzager, Heisenberg, Landau, Kolmogorov, Feynman, and many other great scientists attempted and failed to reach the summit but blazed the trail for the next generations.

Richard Feynman wrote half a century ago in his famous "Lectures in Physics"

"there is a physical problem that is common to many fields, that is very old, and that has not been solved. It is not the problem of finding new fundamental particles, but something left over from a long time ago—over a hundred years. Nobody in physics has really been able to analyze it mathematically satisfactorily in spite of its importance to the sister sciences. It is the analysis of circulating or turbulent fluids."

This analysis aims to properly redefine and solve the Navier-Stokes equations in a limit of vanishing viscosity at fixed energy flow.

In doing so, we must answer some obvious questions.

- *What is the origin of the randomness of the circulating fluid?*
- *Is it spontaneous, and what makes it irreversible?*
- *What are the properties of the fixed manifold covered by this random motion?*
- *Are some "fundamental particles" hidden inside as it was alluded to by Feynman?*

The modern Turbulence theory does not even try to answer these questions.

It resembles the Strong Interaction Theory 60 years ago when I started my scientific career.

Werner Heisenberg promoted an S-matrix dogma, which stated that there was nothing inside the protons, neutrons, and mesons.



Citation: Migdal, A. Title. *Preprints* 2022, 1, 0. <https://doi.org/>

Publisher's Note: MDPI stays neutral with regard to jurisdictional claims in published maps and institutional affiliations.



Copyright: © 2022 by the authors. Licensee MDPI, Basel, Switzerland. This article is an open access article distributed under the terms and conditions of the Creative Commons Attribution (CC BY) license (<https://creativecommons.org/licenses/by/4.0/>).

All particles consisted of each other, and it was FORBIDDEN to ask unobservable questions like "what is inside"?

"Build phenomenological models instead of trying to define and solve the microscopic theory" dictated us the S-matrix dogma.

The Yang-Mills theory already existed but was discarded by Heisenberg and his follower Lev Landau, who declared that

"the Lagrangian is dead and should be buried with all due honors."

Another outstanding mathematical physicist, Sasha Zamolodchikov, recently noted

"they buried the Lagrangian but forgot to drive the stake through its heart."

And then came quarks, gluons, and asymptotic freedom! The rest is history.

We learned that gluon strings confine quarks inside protons and neutrons. We cannot directly observe quarks and gluons, but we can study their almost free motion at small distances inside hadrons.

Quarks and gluons are true fundamental particles, not protons, neutrons, and mesons, as Heisenberg and Landau thought.

0.1. Quarks of Turbulence

In our recent works[1–6], we conjectured that there were confined gauge fields in turbulence, hidden inside the velocity and vorticity fields.

These so-called spherical Clebsch variables are mechanically equivalent to rigid rotators. They are the canonical Hamiltonian variables in the Euler dynamics but cannot propagate as wave excitations.

They play the same role as quarks in the QCD. They are "fundamental particles" inside the turbulent fluid, unobservable in pure form. These spherical Clebsch variables double as gluons, as they are subject to gauge transformations, which leave vorticity and velocity invariant.

These gauge transformations are global in physical space but local in target space (S_2 in this case). These are area-preserving diffeomorphisms or canonical transformations.

This unbroken invariance is the mathematical reason for the Clebsch confinement.

In the same way, as gluons collapse to surfaces bounded by the closed world lines of quarks, these confined variables in turbulent flow collapse into vortex sheets.

The fluctuations of these variables die out in the strong turbulence, echoing the asymptotic freedom. Only three "zero modes" are left, dramatically simplifying the property of the turbulent fixed point.

We have found a Duality of the Turbulence viewed as statistics of the velocity field in R_3 to a quantum mechanical bound state problem in the Loop space.

We cannot yet prove our conjectures and claim that we have reached the shining summit of Turbulence mountain, but we have found a new trail climbing new heights.

Let us give a flyover of this trail before tedious walking step by step.

0.2. Loop Equation and Quantum correspondence

Some lucky nonlinear PDEs in mathematical physics were solved by reduction to a linear problem in a higher dimension.

Some lucky statistical field theories are dual to a fluctuating geometry; strong fluctuations of the original field correspond to weak fluctuations of this geometry.

We say there is double luck with the Navier-Stokes equation. It is equivalent to a large linear problem and dual to weakly fluctuating geometry.

In the Navier-Stokes case, however, we must go up to an infinite-dimensional loop space.

Points in this space are closed loops in 3D space, or the set of three periodic functions $\vec{C}(\theta), \theta \in (0, 2\pi)$.

The linear problem is quantum mechanics in loop space.

This problem is solvable in terms of nonlinear ODE in 1+1 dimensions with random Gaussian initial data [7]; however, this exact singular solution is hard to compute even numerically.

But the strong turbulence corresponds to the WKB limit of the wave function, which is analytically calculable as a fixed point of the loop equation.

0.3. Circulation Intermittency. Area law

The asymptotic solutions of the loop equations [7], which we found in the 90-ties, were impossible to verify at the time with contemporary computer resources.

Besides, they are "too strong to be true," as one respectable mathematical physicist recently told me.

Nobody took seriously the loop equation and its predictions except one persistent man, Katepalli Raju Sreenivasan, who kept trying to verify these predictions for 25 years.

Finally, in 2019, his large-scale simulation [8] confirmed the basic prediction of the loop equation - namely, the Area law.

The Circulation PDF in the inertial region $|\Gamma| \gg \nu$ was a function of the minimal area inside the loop, as we predicted in the 90-ties.

It also decayed exponentially with the circulation, indicating strong intermittency, which was not theoretically explained until recently [4].

In this work, we revise and elaborate on the analysis of that paper.

0.4. Kelvinon. Toroidal Euler vortex with two conserved circulations

The corresponding flow, dominating the fixed point of the Loop equation, was advocated in [4].

Imagine an infinitesimal tube \mathcal{T}_C around fixed spatial loop C . There are two conserved velocity circulations $\Gamma_\alpha, \Gamma_\beta$ around two cycles α, β of this tube as a topological torus. The α cycle goes along the axis of a torus (parallel to C); the β cycle goes around its cross-section (encircling C at some point). Figure 1.

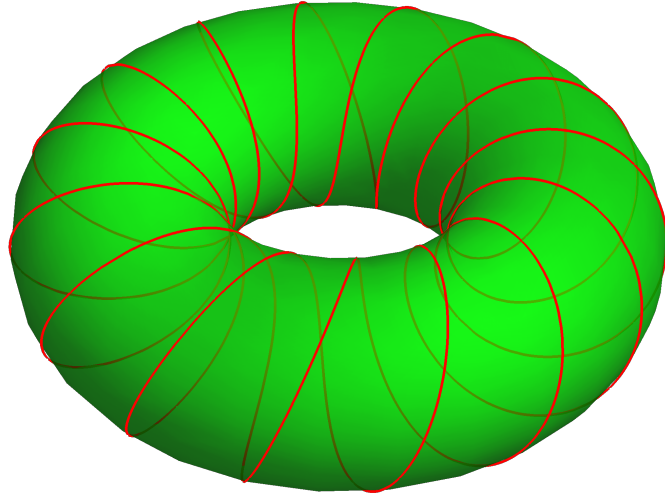


Figure 1. The torus with two cycles .

As we prove below, in the spherical Clebsch variables, these two circulations are quantized

$$\Gamma_\alpha = 4\pi m Z; \quad (1)$$

$$\Gamma_\beta = 4\pi \left(n + \frac{1}{2}\right) Z; \quad (2)$$

$$m \in \mathbb{Z}, n \in \mathbb{Z}; \quad (3)$$

These two cycles in physical space R_3 are mapped by the Clebsch field $ZS_i(\vec{r}), i = 1, 2, 3; \sum S_i^2 = 1$, onto the North pole of the sphere, with circulation proportional to the total area of the sphere 4π

This mapping and the dynamic equations for these Clebsch fields will be described and studied below.

0.5. Anomalous dissipation and anomalous Hamiltonian

The final leg on our trail is related to anomalies coming from short distances, like those in gauge field theories. Our Kelvinon represents a singular solution of the Euler equation, with a singularity at the closed loop.

In the infinitesimal vicinity of this loop, the Euler equation has to be regularized as Navier-Stokes equation.

The solution in this region is given by the Burgers vortex [9]. We match it with the Kelvinon outside this singular core, and in the limit $\nu \rightarrow 0$, we find two anomalies.

One anomaly, implicitly known to Burgers, is anomalous dissipation. In our case of a circular vortex, it results in a beautiful exact formula for the energy dissipation

$$\mathcal{E} = \frac{\Gamma_\beta^2}{8\pi} \oint_C |d\vec{r}| \hat{S}_{tt} \quad (4)$$

where S_{tt} is a projection of the strain $S_{\alpha\beta} = \frac{1}{2}\partial_\alpha v_\beta + \frac{1}{2}\partial_\beta v_\alpha$ on the tangent direction $\vec{t} = d\vec{C}/|d\vec{C}|$ of the loop.

This relation restricts the allowed flows used to minimize the Hamiltonian.

Another anomaly is the regularized term in the Hamiltonian

$$H = \lim_{R \rightarrow 0} \left(\frac{1}{2} \int_{|\vec{r} - \vec{C}| > R} d^3 r \vec{v}^2 + \frac{\Gamma_\beta^2}{8\pi} \oint_C |d\vec{r}| \left(\gamma + \log \frac{S_{tt} R^2}{8\nu} \right) \right); \quad (5)$$

Using the regularized Hamiltonian with the energy flow restriction, we compute its circulation Γ_α in the general form.

6.6. Wilson loop in turbulence

Let us consider the statistical average of the phase factor associated with velocity circulation $\Gamma_\alpha = \oint_C v_\alpha dr_\alpha$

$$\Psi[C, \gamma] = \langle \exp(\iota \gamma \Gamma_\alpha) \rangle \quad (6)$$

In the (Abelian) gauge theory, such an average over quantum fluctuations is called the Wilson loop.

Here, we average over random parameters perturbing the system at spatial infinity.

In the Abelian gauge theory, γ represented electric charge. In our theory, γ has a meaning of the Fourier variable for the velocity circulation.

The Fourier integral of the Wilson loop would produce the circulation PDF

$$P[C, \Gamma] = \int_{-\infty}^{\infty} \frac{d\gamma}{2\pi} \exp(-\iota \gamma \Gamma) \Psi[C, \gamma] \quad (7)$$

The loop equation is derived from the Navier-Stokes equations:

$$\partial_t v_\alpha = \omega_{\alpha\beta} v_\beta - \nu \partial_\beta \omega_{\alpha\beta} - \partial_\alpha \left(p + \frac{1}{2} v_\beta^2 \right); \quad (8)$$

$$\omega_{\alpha\beta} = \partial_\alpha v_\beta - \partial_\beta v_\alpha; \quad (9)$$

$$\partial_\beta v_\beta = 0; \quad (10)$$

The forces can be introduced as a boundary condition for pressure at infinity $p \rightarrow -\vec{f} \cdot \vec{r}$ or as a mean value of the pressure gradient over volume $\vec{f} = -\langle \vec{\nabla} p \rangle_V$. The last expression corresponds to the zeroth Fourier harmonic of $\vec{\nabla} p$.

However, we do not find it useful nor necessary to introduce ad-hoc forces to describe energy flow pumped into our Kelvinon and dissipated at its singular core. Internal sources of randomness are related to the background velocity from the Biot-Savart integrals from far-away vortex structures.

We use this random background velocity as an origin of randomness in the Kelvinon solution.

0.7. Equilibrium Statistics in a Dissipative system

We expect the turbulence phenomenon to be universal up to some phenomenological parameters depending on the definition of the energy pumping.

In the Kolmogorov model, there is only one such parameter $\langle \mathcal{E} \rangle$, the mean energy pumping, but nobody proved that there could not be a few more.

Also, we are interested in the statistical distribution of the turbulent circulation rather than in the kinetic phenomena leading to this equilibrium distribution.

The Navier-Stokes equation is the continuum limit of Newton's mechanics with friction forces described by viscosity and some implicit external forces pumping the energy from the boundary.

Without viscosity, we would have the Gibbs distribution, which results from presumed ergodic motion on the energy surface.

An ergodic hypothesis has not been proven until this day, except in some simple examples.

What can be proven, however, is that the Gibbs distribution represents a fixed point of the evolution equation for the probability distribution of the conservative mechanical system.

In this paper, we shall look only for the equilibrium distribution in the Navier-Stokes as a fixed point of the evolution equation for this dissipative system.

Here is where we radically deviate from the modern Turbulence theory. This theory starts with an (artificial) kinetics, given by forced Navier-Stokes equation.

The true statistical equilibrium could be reached in this theory only after infinite evolution or by ad-hoc averaging over delta-correlated Gaussian forces.

This forced Navier-Stokes equation provides the basis for numerical simulations on a supercomputer, but these simulations have intrinsic noise and approach true equilibrium with error decaying only as $1/\sqrt{t}$.

Worse, this method fails to uncover the properties of this fixed point. What if this fixed point is much simpler than a stochastic trajectory leading to it?

As we all know, the Gibbs distribution $\exp(-\beta E)$ is much simpler than Newton dynamics with stochastic noise in a conservative system.

This stochastic description, though leading to the Gibbs distribution, hides its mathematical beauty behind white noise.

1. The Loop equation and its Fixed Point

Differentiating the Wilson loop functional by time and using the Navier-Stokes equation, we find the identity

$$-i\partial_t \Psi = \gamma \left\langle \oint_C dr_\alpha (v\partial_\beta \omega_{\beta\alpha} - v_\beta \omega_{\beta\alpha}) \exp(i\gamma\Gamma_\alpha) \right\rangle \quad (11)$$

In the papers [10–13], this loop equation (with $\gamma = 1/\nu$) was investigated as a Schrödinger equation in loop space, with the right side replaced by an effective Hamiltonian operator

$$\iota \nu \dot{\Psi}[C] = \mathcal{H}_C \Psi[C]; \quad (12a)$$

$$\mathcal{H}_C = \mathcal{H}_C^{(1)} + \mathcal{H}_C^{(2)} \quad (12b)$$

$$\mathcal{H}_C^{(1)} = -\nu \oint_C dr_\alpha \partial_\beta \hat{\omega}_{\alpha\beta}(r); \quad (12c)$$

$$\mathcal{H}_C^{(2)} = \oint_C dr_\alpha \hat{\omega}_{\alpha\beta}(r) \hat{v}_\beta(r); \quad (12d)$$

$$\hat{\omega}_{\alpha\beta}(\vec{r}) = -\iota \nu \frac{\delta}{\delta \sigma_{\alpha\beta}(\vec{r})}; \quad (12e)$$

$$\hat{v}_\beta(\vec{r}) = \int d^3 \rho \frac{\rho_\gamma}{4\pi |\vec{\rho}|^3} \hat{\omega}_{\beta\gamma}(\vec{r} + \vec{\rho}) \quad (12f)$$

The operator of the area derivative $\frac{\delta}{\delta \sigma_{\alpha\beta}(\vec{r})}$ was defined 40 years ago [14] and then investigated in detail in the gauge theory as well as in the turbulence theory [7,10–13]. We do not need these definitions here, as we will find the fixed point by another method.

We observe viscosity ν appearing in front of time and spatial derivatives, like the Planck constant \hbar in Quantum mechanics. The first term $\mathcal{H}_C^{(1)}$ in our loop Hamiltonian is local in the loop space. The second term $\mathcal{H}_C^{(2)}$ contains the second loop derivatives, acting as a (nonlocal!) kinetic term in loop space.

The loop equation is a particular case of the Hopf equation with a purely imaginary singular source for the velocity field

$$\vec{J}(\vec{r}) = \iota \gamma \int_0^{2\pi} d\theta \vec{C}'(\theta) \delta(\vec{r} - \vec{C}(\theta)) \quad (13)$$

It is a nontrivial property of the Navier-Stokes equation, which allows one to reduce the dimension $3 \Rightarrow 1$ in a Hopf equation.

This functional equation generally depends on the source $\vec{J}(\vec{r})$ for a vector velocity field, mapping $R_3 \mapsto R_3$. The loop functional depends on the loop $\vec{C}(\theta)$, which is a periodic vector field mapping a circle into 3D space $S_1 \mapsto R_3$.

This second term dominates in the WKB limit $\nu \rightarrow 0$, which leads to the Hamilton-Jacobi equation for classical Action $S[C, \gamma]$ our Loop quantum mechanics

$$\oint_C dr_\alpha \omega_{\alpha\beta}^{cl}(r) \int d^3 \rho \frac{\rho_\gamma}{4\pi |\vec{\rho}|^3} \omega_{\beta\gamma}^{cl}(\vec{r} + \vec{\rho}) = 0; \quad (14)$$

$$\omega_{\alpha\beta}^{cl}(r) = \frac{\delta S[C, \gamma]}{\delta \sigma_{\alpha\beta}(\vec{r})}; \quad (15)$$

This WKB equation only defines the C –dependence of the classical action, leaving its γ –dependence arbitrary.

Therefore we could not determine the profile of the circulation PDF, but only the area law:

$$\Psi[C, \gamma] \rightarrow F(\gamma \sqrt{A_C}); \quad (16)$$

$$P[C, \Gamma] = A_C^{-\frac{1}{2}} \Pi \left(\Gamma A_C^{-\frac{1}{2}} \right) \quad (17)$$

Here A_C is the minimal area inside the loop. It was assumed that the contour C is smooth and large compared with viscous scales.

Strictly speaking, it was only proven in quadratic approximation for the minimal surface, which applies to large smooth loops.

Sreenivasan and coworkers [8] confirmed these predictions in large-scale DNS.

2. Kelvinon conjecture

The idea behind our theory is simple: find a solution of the Navier-Stokes equation in the limit of vanishing viscosity such that it conserves the circulation $\Gamma_\alpha(\vec{f})$ around a stationary loop C .

We call such a hypothetical solution a Kelvinon, honoring Kelvin and his famous theorem of conservation of circulation around a liquid loop. Kelvin theorem applies to arbitrary Euler flow, but Kelvinon flow has a particular stagnant loop.

To be more precise, this loop is a closed trajectory of a liquid particle, which makes it stationary as a geometric object. This stationarity is sufficient for the Kelvin theorem leading to conserved circulation.

Then, the Wilson loop will be given by the Gaussian average of $\exp(i\gamma\Gamma_\alpha)$ over some random velocity background to be specified later:

$$\Psi[C, \gamma] = \langle \exp(i\gamma\Gamma_\alpha) \rangle; \quad (18)$$

Finding such a Navier-Stokes solution is easier said than done, but we have a significant simplification. We are looking for the limit of vanishing viscosity.

2.1. The Matching Principle

In this limit, we can use the Euler dynamics everywhere except for some thin boundary regions where large vorticity gradients compensate the viscosity factor in front of this term in the Navier-Stokes equation.

Within the Euler dynamics, boundary regions shrink to lower-dimensional subsets: velocity gap points (shocks) in 1D, point vortexes in 2D, and vortex sheets and vortex lines in 3D.

We have to use full Navier-Stokes equations in these boundary regions. The small thickness of these regions simplifies the geometry of Navier-Stokes equation: we can neglect all the curvature effects.

These flat (or straight line) Navier-Stokes solutions must match the Euler solution outside the boundary regions. Thus, the Navier-Stokes provides the boundary condition to Euler and vice versa.

This matching principle was suggested in our recent work [5,6] and applied to the Euler vortex sheets (tangent velocity gaps in purely potential flow).

In general, the matching principle removes the ambiguity of the weak solutions of the Euler dynamics by resolving the singularities at surfaces and lines.

It also let one select among the various exact solutions of the Navier-Stokes equations in a flat geometry.

The matching conditions led to so-called CVS equations [5,6] for the stable vortex sheets (velocity gaps in potential flow). The vortex sheets bounded by a fixed loop do not belong to that category.

As we shall see, a line singularity is also required at the loop, making it a Dirac monopole of the Euler equation.

2.2. Dirac monopole line with Burgers vortex at the core

Figure 2.

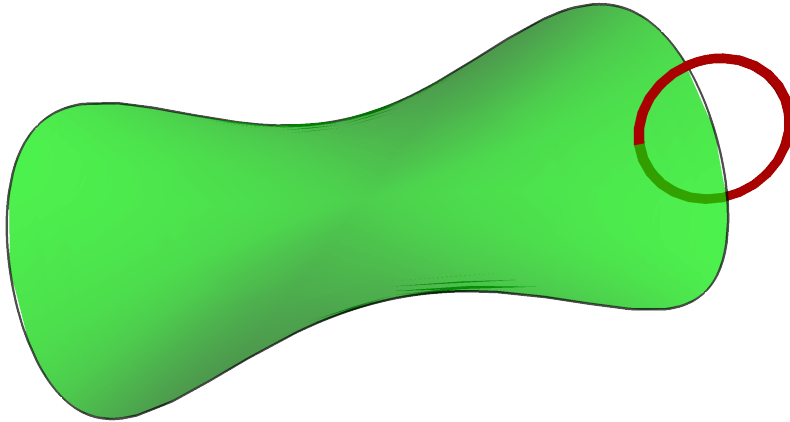


Figure 2. Kelvinon cycles. The β cycle (red) around the α cycle (black) of the vortex sheet (green).

Let us consider (yet to be determined) Euler flow with a singular vortex line at the smooth loop C . We surround this loop with a thin tube; its radius varies around the loop and must be much smaller than its local curvature radius.

Let us first consider the core, which we assume is a cylindrical region, given its small radius. We assume cylindrical symmetry and take the Burgers vortex solution [9] of the Navier-Stokes equation.

$$\vec{v} = \{-\alpha x - g(r)y, -\alpha y + g(r)x, 2\alpha z\}; \quad (19)$$

$$g(r) = \frac{\left(1 - e^{-\frac{\alpha r^2}{2\nu}}\right)\Gamma_\beta}{2\pi r^2}; \quad (20)$$

$$r = \sqrt{x^2 + y^2}; \quad (21)$$

$$\Gamma_\beta = \oint_{\beta} \vec{v} \cdot d\vec{r}; \quad (22)$$

$$\alpha = \frac{1}{2} \hat{t} \cdot \hat{S} \cdot \hat{t}; \quad (23)$$

$$\hat{t} = \{0, 0, 1\} \quad (24)$$

Here $\hat{S}_{\alpha\beta} = \frac{1}{2}(\partial_\alpha v_\beta + \partial_\beta v_\alpha)$ is the strain tensor far away from the center of the core, and \vec{t} is the local tangent vector of the loop (the axis of a cylindrical tube).

Γ_β is the velocity circulation around the cylinder cross-section far away from its axis (the β cycle of the tube).

These two parameters Γ_β, α have to be matched by an Euler solution at the surface of the tube.

The contribution to the Euler Hamiltonian from the cross-section of the circular core of the vortex at $z = 0$ is computed using *Mathematica*[®]

$$\begin{aligned} \frac{1}{2} \int_{x^2+y^2 < R^2} dx dy \vec{v}(x, y, 0)^2 = \\ \frac{\Gamma_\beta^2}{8\pi} \left(\gamma + \log \left(\frac{\alpha R^2}{4\nu} \right) \right) + \frac{1}{4} \pi \alpha^2 R^4 + \\ \frac{\Gamma_\beta^2}{4\pi} \left(\text{Ei} \left(-\frac{R^2 \alpha}{\nu} \right) - \text{Ei} \left(-\frac{R^2 \alpha}{2\nu} \right) \right) \end{aligned} \quad (25)$$

where $\text{Ei}(x)$ is an exponential integral function.

In the turbulent limit $\nu \rightarrow 0$ we get

$$\frac{\Gamma_\beta^2}{8\pi} \left(\gamma + \log \left(\frac{\alpha R^2}{4\nu} \right) \right) + \frac{1}{4} \pi \alpha^2 R^4 + O \left(\exp \left(-\frac{R^2 \alpha}{2\nu} \right) \right) \quad (26)$$

The quadratic terms are also negligible in our approximation $R \rightarrow 0$. Now, the total contribution from the tube around the loop will be

$$\frac{1}{2} \int_{|\vec{r} - \vec{C}| < R} d^3 r \vec{v}^2 \rightarrow \frac{\Gamma_\beta^2}{8\pi} \oint_C |d\vec{r}| \left(\gamma + \log \frac{\alpha R^2}{4\nu} \right); \quad (27)$$

We have the following form of the total Hamiltonian for the Euler flow

$$H = \frac{1}{2} \int_{|\vec{r} - \vec{C}| > R} d^3 r \vec{v}^2 + \frac{\Gamma_\beta^2}{8\pi} \oint_C |d\vec{r}| \left(\gamma + \log \frac{\alpha R^2}{4\nu} \right); \quad (28)$$

This Hamiltonian must be minimized within the topological class of flows with fixed circulations $\Gamma_\alpha, \Gamma_\beta$.

As for the dissipation in the Burgers vortex, it is finite in the turbulent limit. The vorticity vector

$$\vec{\omega} = \left\{ 0, 0, \frac{\alpha \Gamma_\beta e^{-\frac{\alpha(x^2+y^2)}{2\nu}}}{2\pi\nu} \right\} \quad (29)$$

and the enstrophy integral

$$\int_V d^3 r \vec{\omega}^2 = \frac{\Gamma_\beta^2}{4\pi\nu} \oint_C |d\vec{r}| \alpha \left(1 - e^{-\frac{\alpha R^2}{\nu}} \right) \quad (30)$$

In the turbulent limit, $\nu \rightarrow 0$, we find finite energy dissipation due to our circular Burgers vortex

$$\mathcal{E}_d = \nu \int_V d^3 r \vec{\omega}^2 \rightarrow \frac{\Gamma_\beta^2}{4\pi} \oint_C d\theta \alpha; \quad (31)$$

$$\vec{C}'(\theta)^2 = 1; \quad (32)$$

$$\alpha = \frac{1}{2} \left(\vec{C}'(\theta) \cdot \vec{\nabla} \right) \left(\vec{v} \cdot \vec{C}'(\theta) \right); \quad (33)$$

The Burgers solution has the strain nonsingular and constant at the loop, but this constant tensor is not the most general one. There is an extra restriction on the strain tensor at the loop.

$$S_{nn} = -\frac{1}{2}S_{tt}. \quad (34)$$

Here S_{nn} is the normal (i.e., radial) component of the local strain at some point of the loop, and S_{tt} is as, before, the tangent projection along the loop.

This restriction is a particular case of the boundary conditions imposed on the Euler flow by matching it with the Navier-Stokes solution in the core of the singular loop.

2.3. Faddeev parametrization and the Kelvinon topology

The parameterization of vorticity, allowing our topology, was first suggested by Ludwig Faddeev and applied in [15,16] for computation of the simplest topological invariant: the helicity of Euler flow on a closed Riemann sphere S_3 . It was reduced to the Hopf invariant, well-known in topology.

The Faddeev parametrization (or spherical Clebsch variables) was applied to the turbulence problem in our recent works, starting with [3].

$$\vec{\omega} = Ze_{abc}S_a \vec{\nabla} S_b \times \vec{\nabla} S_c; \quad (35)$$

$$S_1^2 + S_2^2 + S_3^2 = 1; \quad (36)$$

where Z is some global constant with the dimension of viscosity, which becomes an **integral of motion** in Euler dynamics.

The Poisson brackets for these three components of the unit vector \vec{S} is equivalent to the rigid rotator

$$[S_a(\vec{r}), S_b(\vec{r}')] = \delta(\vec{r} - \vec{r}')e_{abc}S_c(\vec{r}); \quad (37)$$

$$[S_a(\vec{r}), H] = -\vec{v}(\vec{r}) \cdot \vec{\nabla} S_a(\vec{r}); \quad (38)$$

$$H = \frac{1}{2} \int d^3r \vec{v}^2 \quad (39)$$

One can introduce two canonical Clebsch variables as

$$\phi_1 = Z(1 + S_3); \quad (40)$$

$$\phi_2 = \arg(S_1 + iS_2) \quad (41)$$

$$\vec{\omega} = \vec{\nabla} \phi_2 \times \vec{\nabla} \phi_1 \quad (42)$$

Then the Poisson brackets will be the same as those for the coordinate and momentum of the harmonic oscillator

$$[\phi_i, \phi_j] = Z\delta(\vec{r} - \vec{r}')e_{ij}; \quad (43)$$

However, these variables are constrained, plus ϕ_2 is defined modulo 2π . Thus, the target space of these fields $\phi_i(\vec{r})$ is still a sphere S_2 .

These are internal coordinates (related to Euler angles) on this sphere. Observables, such as vorticity and velocity, do not depend on the choice of internal coordinates in the target space.

The vorticity is invariant under local symplectic transformations in the target space

$$\delta\phi_i = e_{ij} \frac{\partial h(\phi_1, \phi_2)}{\partial \phi_j}; \quad (44)$$

$$\delta S_a = e_{ij} \frac{\partial S_a}{\partial \phi_i} \frac{\partial h(\phi_1, \phi_2)}{\partial \phi_j}; \quad (45)$$

$$\delta\vec{\omega} = 0 \quad (46)$$

Their motion compact and leads to some winding numbers related to mapping the physical space to S_2 .

In our case, the physical space \mathcal{P} is the whole space R_3 without an infinitesimal tube \mathcal{T} around the loop C and without the discontinuity surface S_C without its boundary C .

$$\mathcal{P} = R_3 / (\mathcal{T} \oplus S_C / C) \quad (47)$$

At this surface S_C , the angular variable ϕ_2 has $2\pi(n + \frac{1}{2})$ discontinuity, with integer n .

Consequently, $\psi \equiv S_1 + iS_2$ changes the sign

$$\psi^-(S_C) = \psi^+(S_C) e^{i\pi(2n+1)}; \quad (48)$$

$$\psi^-(S_C) + \psi^+(S_C) = 0 \quad (49)$$

Consequently, this complex variable ψ must vanish at C .

We arrive at the boundary condition

$$S_a(C) = \delta_{a3}; \quad (50)$$

$$\phi_1(C) = 2Z \quad (51)$$

Our physical space \mathcal{P} is topologically equivalent to a full 3D torus. The Clebsch field maps $\mathcal{P} \mapsto S_2$; two winding numbers describe this mapping.

The velocity field can be written as the Biot-Savart integral

$$\vec{v} = Z\tilde{v}; \quad (52)$$

$$\vec{\omega} = Z\tilde{\omega}; \quad (53)$$

$$\tilde{\omega} = e_{abc} S_a \vec{\nabla} S_b \times \vec{\nabla} S_c; \quad (54)$$

$$\tilde{v} = \vec{\nabla} \Phi - \vec{\nabla} \times \vec{\Psi}; \quad (55)$$

$$\vec{\Psi}(\vec{r}) = \int d^3 r' \frac{\tilde{\omega}(\vec{r}')}{4\pi|\vec{r} - \vec{r}'|}; \quad (56)$$

$$\tilde{v}_n(S_C) = 0; \quad (57)$$

The potential Φ satisfies the Laplace equation with the Neumann boundary condition at S_C / C to cancel the normal velocity coming from the $\vec{\nabla} \times \vec{\Psi}$ term in the Biot-Savart law. One can prove that the normal derivative of this term is continuous at the surface, so the potential term $\vec{\nabla} \Phi$ has to cancel continuous normal velocity at the surface.

There is also a boundary condition at the loop $C = \partial S_C$, following from the matching condition (34):

$$2\partial_n^2 \Phi(C) + \partial_t^2 \Phi(C) = 0; \quad (58)$$

This restriction does not affect the rotational part of velocity, which is fixed by the circulation $\Gamma_\beta = 4\pi\left(n + \frac{1}{2}\right)$.

At the surface S_C/C , there is only a tangent discontinuity of velocity coming from the delta function in vorticity. The boundary values are

$$\vec{\omega} \rightarrow 2\pi\left(n + \frac{1}{2}\right)Z\delta(z)\vec{\sigma} \times \vec{\nabla}S_3; \quad (59)$$

$$\vec{v}^+ - \vec{v}^- = 2\pi\left(n + \frac{1}{2}\right)Z\vec{\nabla}S_3; \quad (60)$$

$$S_3^+ = S_3^-; \quad (61)$$

$$\phi_2^+ = \phi_2^- - 2\pi\left(n + \frac{1}{2}\right); \quad (62)$$

$$\omega_n^+ = \omega_n^- = Ze_{ij}\partial_i\phi_2^\pm\partial_jS_3^\pm \quad (63)$$

Here $\vec{\sigma}$ is the local normal vector to the surface, and z is the normal coordinate at this point.

The circulation at the α, β cycles is calculable in terms of these two winding numbers as we have quoted in (1).

The following steps lead to these formulas

$$\Gamma_\alpha = \oint_\alpha v_\alpha dr_\alpha = \int_{S_C^+} d\vec{\sigma} \cdot \vec{\omega}^+ = \int_{S_C^+} d\phi_1 \wedge d\phi_2 = \int_\alpha \phi_1 d\phi_2 = 4\pi m Z; \quad (64)$$

$$\Gamma_\beta = \oint_\beta v_\alpha dr_\alpha = - \oint_\beta \phi_1 d\phi_2 = 4\pi\left(n + \frac{1}{2}\right)Z; \quad (65)$$

We took advantage of the boundary value $\phi_1(C) = 2Z$.

We conclude that the circulation Γ_α around the initial loop C is related to the integral of Euler motion Z times integral winding number m .

Is such a topology even possible? We have built an example of the Clebsch field with two winding numbers and proper boundary conditions at the surface and infinity.

This example is presented in Appendix A. It could be used as a zeroth approximation to minimize our renormalized Hamiltonian by relaxation.

2.4. The energy flow balance and energy minimization

By definition, the time derivative of any functional of the velocity satisfying the stationary Navier-Stokes equations must vanish.

Let us consider the time derivative of the Hamiltonian in our space (47) and use Navier-Stokes equation to reduce it to an integral of the divergence of an energy current

$$0 = \partial_t H = \int_{\mathcal{P}} \vec{v} \cdot \partial_t \vec{v} = \int_{\mathcal{P}} \vec{\nabla} \cdot \vec{J}; \quad (66)$$

$$\vec{J} = \left(p + \frac{\vec{v}^2}{2}\right)\vec{v} + \nu\vec{\omega} \times \vec{v} \quad (67)$$

By the Stokes theorem, this integral reduces to the sum of a flux of this current through the external and internal boundaries of our space

$$0 = \int_{\partial_{-\mathcal{P}}} J_n + \int_{\partial_{+\mathcal{P}}} J_n; \quad (68)$$

$$\partial_{-\mathcal{P}} = \mathcal{T} \oplus \mathcal{S}_C/C; \quad (69)$$

$$\partial_{+\mathcal{P}} = \mathcal{B} \quad (70)$$

Here \mathcal{B} is some surface surrounding our loop C far away from it. The flux through this boundary \mathcal{B} represents the incoming energy flow \mathcal{E}_p pumping energy from other vortex structures in the infinite volume.

We arrive at the identity, relating this energy flow \mathcal{E}_p to the flux of the same energy current through the inner boundary

$$-\mathcal{E}_p = \int_{\mathcal{S}_C/C} J_n + \int_{\mathcal{T}} J_n \quad (71)$$

Here the normal vector points from the physical space inside the tube at its surface. Unlike the flux through the external boundary, this equal flux is related to our Kelvinon solution.

At the discontinuity surface \mathcal{S}_C/C , the normal velocity vanishes on our Kelvinon solution. The second term

$$\mathcal{J}_n = \nu(\vec{\omega} \times \vec{v})_n \quad (72)$$

is not zero, but it vanishes in the turbulent limit. At finite ν , it must match the surface dissipation

$$\nu \int_{-\infty}^{\infty} dz \vec{\omega}_{NS}^2 \quad (73)$$

where z is the local normal coordinate to the surface, and ω_{NS} is the Navier-Stokes solution for the vortex sheet vorticity in the viscous layer.

We are not interested in the balance of these terms, as they vanish in the turbulent limit.

We are left with the integral over the surface of our infinitesimal tube \mathcal{T} . Simple calculation with the Burgers vortex yields $v_n = \alpha R$. The integral over the circle of $\nu \vec{v} \times \vec{\omega}$ was computed using *Mathematica*[®]. In the limit $R \rightarrow 0$, we find finite result

$$\mathcal{E}_p = \frac{\Gamma_\beta^2}{4\pi} \oint_C |d\vec{r}| \alpha \quad (74)$$

As expected, this is the same as the dissipation. This coincidence means we have correctly used the Burgers vortex in the limit of $R \rightarrow 0$.

Now we can relate the energy flow to the parameters of the Kelvinon.

$$\mathcal{E}_p = \mathcal{E}_d \equiv \mathcal{E} = \frac{\Gamma_\beta^2}{4\pi} \oint_C |d\vec{r}| \alpha \quad (75)$$

Finite anomalous dissipation on a circular Burgers vortex, matching the energy flow from spacial infinity, is what Burgers dreamed up in his pioneering work.

This equation reflects the energy conservation in the stationary solution of the full Navier-Stokes equation. According to our Matching Principle, we have to add this constraint to the Energy minimization of the Euler Hamiltonian, with anomalies taken into account.

Expressed in terms of Faddeev variables, velocity, and vorticity fields are proportional to Z as in (55)

$$\Gamma_\beta = 4\pi \left(n + \frac{1}{2} \right) Z; \quad (76)$$

$$\alpha = Z\tilde{\alpha}; \quad (77)$$

$$\tilde{\alpha} = \frac{1}{2} \left(\vec{t} \cdot \vec{\nabla} \right) (\tilde{v} \cdot \vec{t}); \quad (78)$$

$$\vec{t} = \frac{d\vec{C}}{|d\vec{C}|} \quad (79)$$

The parameter Z along with the vector field $\vec{S}(\vec{r})$ must be found from the minimization of the Hamiltonian with an extra constraint of energy conservation

$$H_R = Z^2 A[\tilde{v}] + BZ^2 \left(\gamma + \log \frac{Z}{4\nu} \right) + \lambda \left(4\pi \left(n + \frac{1}{2} \right)^2 Z^3 \oint_C |d\vec{r}| \tilde{\alpha} - \mathcal{E} \right) + \oint_C d\theta |\vec{C}'(\theta)| \mu(\theta) (\tilde{S}_{nm} + \tilde{\alpha}); \quad (80)$$

$$A[\tilde{v}] = \lim_{R \rightarrow 0} \left(\frac{1}{2} \int_{|r-C|>R} \tilde{v}^2 + 2B \log R \right) + 2\pi \left(n + \frac{1}{2} \right)^2 \oint_C |d\vec{r}| \log \tilde{\alpha}; \quad (81)$$

$$B = 2\pi \left(n + \frac{1}{2} \right)^2 |C|; \quad (82)$$

The minimization by Lagrange multiplier $\mu(\theta)$ yields the boundary condition on potential part Φ at the loop, following from the matching with Burgers vortex.

The minimization by Lagrange multiplier λ leads to an equation for Z

$$Z = \left(\frac{\mathcal{E}}{4\pi \left(n + \frac{1}{2} \right)^2 \oint_C |d\vec{r}| \tilde{\alpha}} \right)^{\frac{1}{3}} \quad (83)$$

The renormalized velocity \tilde{v} minimizes the reduced Hamiltonian H_R by its parameters, (\vec{S}, λ, Z)

$$(\vec{S}, \lambda, Z) = \arg \min_{\vec{S}, \lambda, Z} H_R; \quad (84)$$

$$\tilde{v} = \tilde{v}[S]; \quad (85)$$

The spurious parameter R , which formally enters this Hamiltonian, drops from it in the limit $R \rightarrow 0$. The singular terms in the integral over external region $|\vec{r} - \vec{C}| > R$ exactly cancel the logarithmic term $2B \log R$ leaving the finite limit.

This can be proven by differentiating the reduced Hamiltonian by $\log R$, which selects the lower limit of the radial integration in the $\int_{|r-C|>R} \tilde{v}^2$. We get velocity square at the surface of

the tube, where it is dominated by the singular vortex with circulation $4\pi\left(n + \frac{1}{2}\right)$. Adding both terms, we obtain zero in the limit of $R \rightarrow 0$.

$$\begin{aligned} R\partial_R \left(4\pi\left(n + \frac{1}{2}\right)^2 |C| \log R + \int_{|r-C|>R} d^3\vec{r} \frac{\tilde{v}^2}{2} \right) \rightarrow \\ 4\pi\left(n + \frac{1}{2}\right)^2 |C| - \oint_C |d\vec{r}| \int_0^{2\pi} d\theta R^2 \frac{2\left(n + \frac{1}{2}\right)^2}{R^2} = 0 \end{aligned} \quad (86)$$

However, in that limit, there is so-called dimensional transmutation.

The constant term arising after the cancellation of logarithmic terms $\log R$ has a logarithmic dimension. The solution for reduced velocity \tilde{v} has an arbitrary parameter of the dimension of length, which parameter takes care of this logarithmic dimension.

This parameter compensates for the logarithmic dimension of the last term $\propto \oint_C |d\vec{r}| \log \tilde{\alpha}$ in the reduced Hamiltonian.

2.5. Random boundary conditions

Our Kelvinon does not live in isolation; there are other vortex bubbles (other Kelvinons?) in the fluid. We assume these other bubbles to be far away, so we do not need to specify their structure.

The parameter \mathcal{E} represents the net energy flow from these other structures through the large sphere \mathcal{B} surrounding our Kelvinon. As such, this parameter does not depend on the geometry or parameters of the Kelvinon. In particular, it does not depend on the loop C .

It depends on small random background velocity \vec{v}_0 at the boundary \mathcal{B} . This random background velocity is related to the random positions and orientations of other Kelvinons. The Biot-Savart tails decay as $1/r^3$, which makes them very small, but there is a large number $O(r^3)$ of those structures like stars in the "night sky paradox." They would then add up to a random constant background velocity, distributed as a Gaussian by the CLT.

In general, we expect the local value of the energy pumping flow \mathcal{E} to be equal to some constant part, plus some smaller part related to these random background velocity

$$\mathcal{E} \approx \langle \mathcal{E} \rangle + \vec{v}_0 \cdot \hat{Q} \cdot \vec{v}_0 - \sigma \text{tr } Q; \quad (87)$$

$$\vec{v}_0 \sim \mathcal{N}(0, \|\sigma \delta_{\alpha\beta}\|) \quad (88)$$

The constant parameter $\langle \mathcal{E} \rangle$ represents the mean value of energy flow.

The linear term is missing by parity (not isotropy, which is generally valid only in average).

We assume that the fluctuating part is much smaller than the mean value of the energy flow, i.e.

$$\sigma \hat{Q} \ll \langle \mathcal{E} \rangle \quad (89)$$

In that approximation, we get for Z

$$Z = Z_0[C](1 + \vec{v}_0 \cdot \hat{Q} \cdot \vec{v}_0 - \sigma \text{tr } \hat{Q}); \quad (90)$$

$$Z_0[C] = \left(\frac{\langle \mathcal{E} \rangle}{4\pi\left(n + \frac{1}{2}\right)^2 \oint_C |d\vec{r}| \tilde{\alpha}} \right)^{\frac{1}{3}}; \quad (91)$$

$$\hat{Q} = \frac{\hat{Q}}{3\langle \mathcal{E} \rangle} \quad (92)$$

Assuming we know $\tilde{\alpha}$, which is a formidable but well-defined minimization problem, we can now write down the Wilson loop as follows

$$\Psi[C, \gamma] = \langle \exp(4\pi m i \gamma Z_0[C](1 + \vec{v}_0 \cdot \hat{q} \cdot \vec{v}_0 - \sigma \text{tr } \hat{q})) \rangle_f = \frac{\exp(i\tau\gamma)}{\sqrt{\det(1 - i\gamma\hat{\Lambda})}}; \quad (93)$$

$$\tau = 4\pi m Z_0[C](1 - \sigma \text{tr } \hat{q}); \quad (94)$$

$$\hat{\Lambda} = 8\pi m Z_0[C]\sigma \hat{q}; \quad (95)$$

The PDF is given by the integral over the quadratic surface

$$P[C, \Gamma] = \int \frac{d^3 \vec{\xi}}{(2\pi)^{\frac{3}{2}}} \exp\left(-\frac{\vec{\xi}^2}{2}\right) \delta\left(\Gamma - \tau - \vec{\xi} \cdot \hat{\Lambda} \cdot \vec{\xi}\right) \quad (96)$$

The quadratic surface $\Gamma = \tau + \vec{\xi} \cdot \hat{\Lambda} \cdot \vec{\xi}$ is not closed, because the matrix $\hat{\Lambda}$ is not positive definite. This is rather a hyperbolic surface, extending to infinity. The Gaussian factor provides the convergence.

3. Comparison with Numerical experiments

These formulas are ridiculously simple.

Where are the multi-fractal scaling and all other scary complications?

The short answer is that this is the equilibrium statistical average in the **strong turbulence** regime; this regime has not been observed in most of the physical and numerical experiments.

The longer answer is as follows. Only the recent large-scale simulations on a supercomputer [8,17] gave us a glimpse of the strong turbulence. In our opinion, the multi-fractal phenomena are a transient regime preceding strong turbulence.

The authors of [18], [19] expressed a similar opinion that there was a "fourth turbulence phase" where the exponents of the multi-fractal scaling laws saturate at simple limits, reflecting some coherent vortex structure.

Our opinion is stronger than that. We do not see any theoretical grounds for scale or conformal invariance in a nonlocal system described by the Navier-Stokes or Euler equation. The multi-fractal scaling laws are a general mathematical framework capable of approximating many natural phenomena.

So, we see these scaling laws as a compact way to describe the transient regime between weak and strong turbulence rather than an exact asymptotic scale invariance with anomalous dimensions. There must be some systematic deviations from the straight lines in the log-log plot of the moments of velocity difference vs. the separation size.

We do not insist on that opinion but rather request a larger and more precise measurement of the curvature of this log-log plot to verify the multi-fractal scaling laws.

We took the data from [8] (courtesy of Kartik Iyer) and plotted them in a different way, not assuming the multi-fractal scaling laws. The errors are most likely artifacts of random forcing at an 8K cubic lattice¹. The prediction $\Gamma \sim \sqrt{\text{area}}$ of the loop equations perfectly fits the DNS, without any assumptions of multi-fractal scaling laws. Figure 3.

¹ This is not to say that some other nonlinear formulas cannot fit this data equally well or maybe even better, for example, fitting $\log S$ by $\log R$ would produce a very good linear fit with the slope 1.1 instead of our 1. Data fitting cannot derive the physical laws – it can only verify them against some null hypothesis

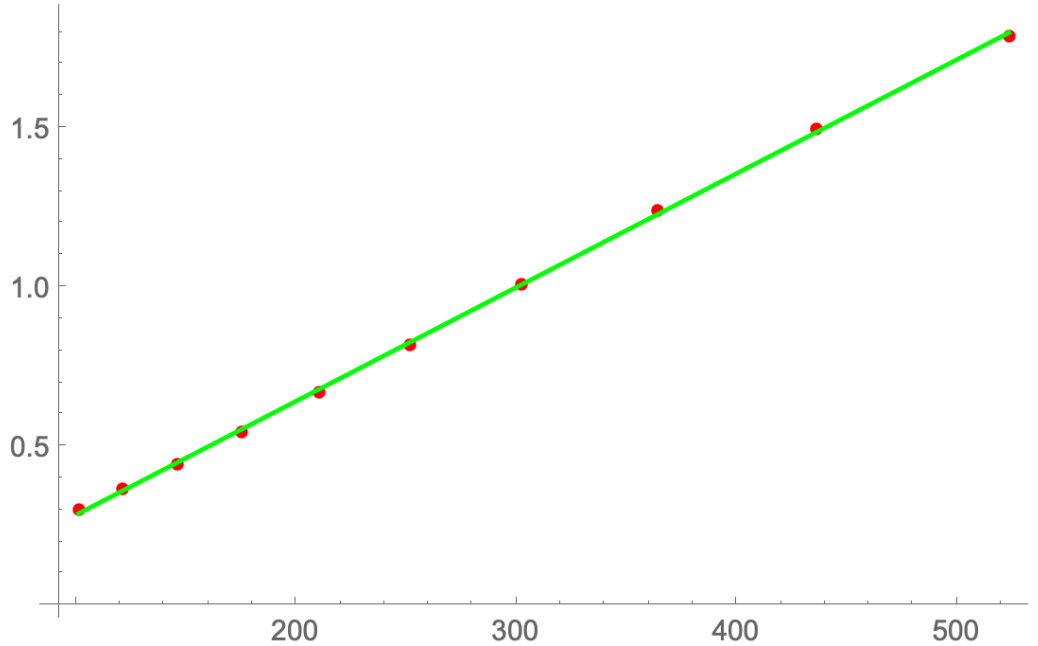


Figure 3. Linear fit of the circulation scale $S = \sqrt{\frac{M_8}{M_6}}$ (with $M_p = \langle \Gamma^p \rangle$) as a function of the a/η for inertial range $100 \leq a/\eta \leq 500$. Here a is the side of the square loop C , and η is a Kolmogorov scale. The linear fit $S = -0.073404 + 0.00357739a/\eta$ is almost perfect: adjusted $R_2 = 0.999609$.

Final comment. This transient regime leading to strong turbulence may look quite complex when one studies stochastic processes designed to imitate statistical equilibrium. However, the mathematical properties of this equilibrium in the limit of strong turbulence could be as simple as $\exp(-\beta H)$.

The complexity of a particular computational method (forced Navier-Stokes equations in this case) does not preclude the answer from being simple.

For example, in the 1D Burgers equation, the answer was a simple distribution of velocity difference $\theta(\Delta v) \exp(-a\Delta v^3)$ despite the complexity of the instanton analysis[20] and dual analysis [21] of the dynamics of the shocks.

Apropos, the analysis of [21] dealt with anomalous dissipation in the 1D Burgers model, and it was an essential part of the master equation studied there. This master equation was a 1D analog of the loop equation [7] without the incompressibility condition.

Coming back to 3D, let us first check how this impossible formula compares to the numerical experiment.

Remember that we took an extreme turbulence limit $\nu \rightarrow 0$ at fixed $\langle \mathcal{E} \rangle$.

In the real world, with finite viscosity and finite volume, we could only match the predictions of our theory for the tails of the PDF $P[C, \Gamma]$, where the Reynolds number $|\Gamma|/\nu$ is large.

In particular, we cannot match the low moments of the circulation, corresponding to low coefficients of the Taylor expansion of the Wilson loop

$$\frac{\exp(i\gamma\tau)}{\sqrt{\det(1 - i\gamma\hat{\Lambda})}} = \sum_{r=0}^{\infty} \frac{(i\gamma)^r}{n!} M_r[C]; \quad (97)$$

$$M_r[C] = \langle \Gamma_\alpha^r \rangle \quad (98)$$

The highest moments are related to the PDF tails so that they can be compared with DNS.

We have computed the asymptotics of the higher moments of this algebraic function. However, comparing these PDF tails is better, as they were measured in [8,17] with great precision over 15 decades of probability.

The highest moments are mathematically related to the PDF tails, so they do not add new information.

3.1. PDF tails and time symmetry breaking

The asymptotic tails of the PDF can be easiest to compute from the integral representation

$$P[C, \Gamma] = \int_{-\infty}^{\infty} dt \int_{-i\infty}^{i\infty} dx \frac{1}{2\pi\sqrt{\pi}} \exp\left((\tau - \Gamma)x - t^2(1 - ax)(1 - bx)(1 - cx)\right) \quad (99)$$

where $x = i\gamma$ and $a > b > 0, c < 0$ are eigenvalues of $\hat{\Lambda}$, in decreasing order.

The saddle point computation chooses one of the six saddle points in the complex plane. Let us first consider the case of positive large Γ . The relevant point in this case is

$$\left\{ x = \frac{1}{a}, t = \frac{\sqrt{a(-\tau + \Gamma)}}{\sqrt{(a-b)(a-c)}} \right\}, \quad (100a)$$

$$P(C, \Gamma \rightarrow +\infty) \rightarrow \frac{\exp\left(\frac{\tau - \Gamma}{a}\right)}{2\sqrt{\pi} \sqrt{\frac{(a-b)(a-c)\Gamma}{a}}} \quad (100b)$$

Likewise, in the case of large negative Γ

$$\left\{ x = \frac{1}{c}, t = \frac{\sqrt{c(-\tau + \Gamma)}}{\sqrt{(c-a)(c-b)}} \right\}; \quad (101a)$$

$$P(C, \Gamma \rightarrow -\infty) \rightarrow \frac{\exp\left(\frac{\tau - \Gamma}{c}\right)}{2\sqrt{\pi} \sqrt{\frac{(a-c)(b-c)\Gamma}{c}}} \quad (101b)$$

We observe the explicit breaking of the time-reversal symmetry in the turbulent region $|\Gamma| \gg \nu$. This breaking comes from the time-odd winding number m of the Kelvinon. With the anti-Kelvinon, we would have the PDF reflected $\Gamma \Rightarrow -\Gamma$.

We have the Stokes phenomenon from the point of view of the loop equation analysis. Two analytic functions give the asymptotic behavior at the positive and negative Γ .

This phenomenon resolves the paradox of Sasha Polyakov, who objected to the early version of the Area law on the following grounds. The Minimal area is invariant against the orientation reversal of the loop, as opposed to circulation, which changes its sign. The PDF must be an even function of the ratio of Γ to any function of the minimal area.

We now see two asymptotic solutions to the loop equation: one for positive and another for negative circulation.

The orientation reversal does not continue one asymptotic solution into another because of the Stokes phenomena in our integral representation (99).

We also see that for the non-planar loop C , the dependence of its shape is more complex than just the minimal area, though the discontinuity surface still coincides with the minimal surface.

These asymptotic PDF tails are the missing piece of our fixed point theory based on loop equations. In particular, the vorticity correlations at the vortex surface expressed in that PDF[12] are now completely specified.

3.2. Matching the Kelvinon solution to the DNS

Let us compare these relations to DNS[8], courtesy of Kartik Iyer.

This raw data correspond to 8192^3 DNS with $R_\lambda = 1300$. There are the first 8 moments of circulation for various Reynolds numbers.

The PDF data for velocity circulation corresponds to $r/\eta \approx 140$. The circulation is measured in viscosity ν (here, we restored the correct normalization of circulation, which was lost in [8] where circulation was measured in some arbitrary units).

This data is the most extensive, with circulation $-1904.72 < \Gamma < 2048.47$. We discarded the extreme values, as the statistics were too small there.

The small absolute values of Γ were also discarded, as our theory only applies to large $|\Gamma|$. We selected the interval $610 < |\Gamma| < 1426$ corresponding to probabilities $10^{-7} > P > 10^{-14}$ and we fitted

$$\log\left(P(C, \Gamma)\sqrt{|\Gamma|}\right) \approx A_\pm + B_\pm|\Gamma|; \quad (102)$$

$$(B_+, B_-) = (-1/a, 1/c); \quad (103)$$

Figure 4.

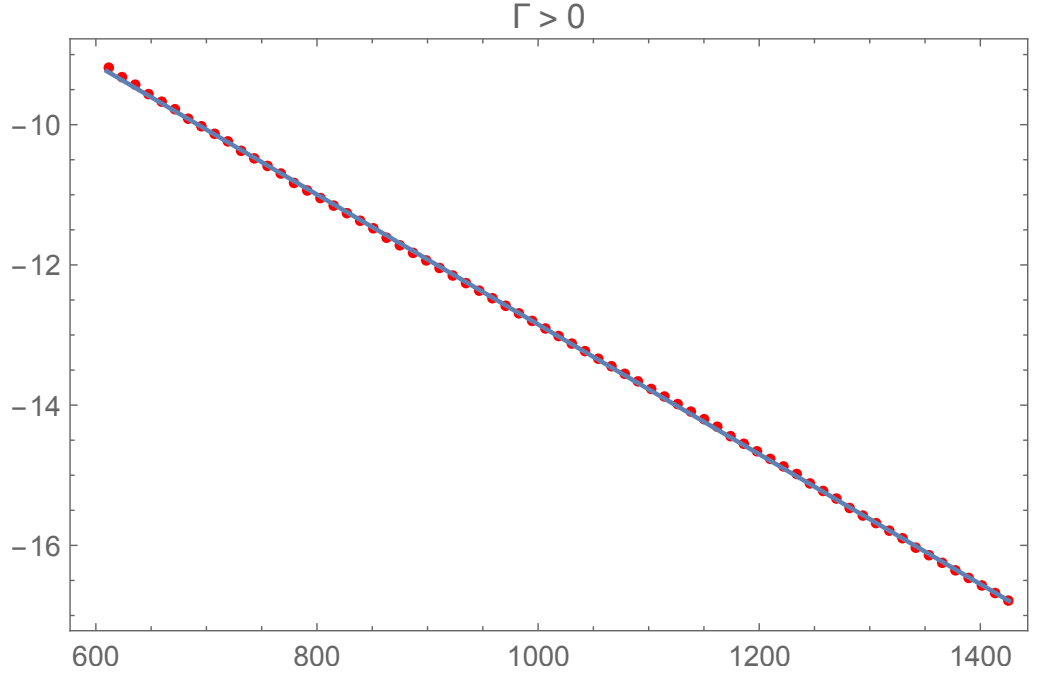
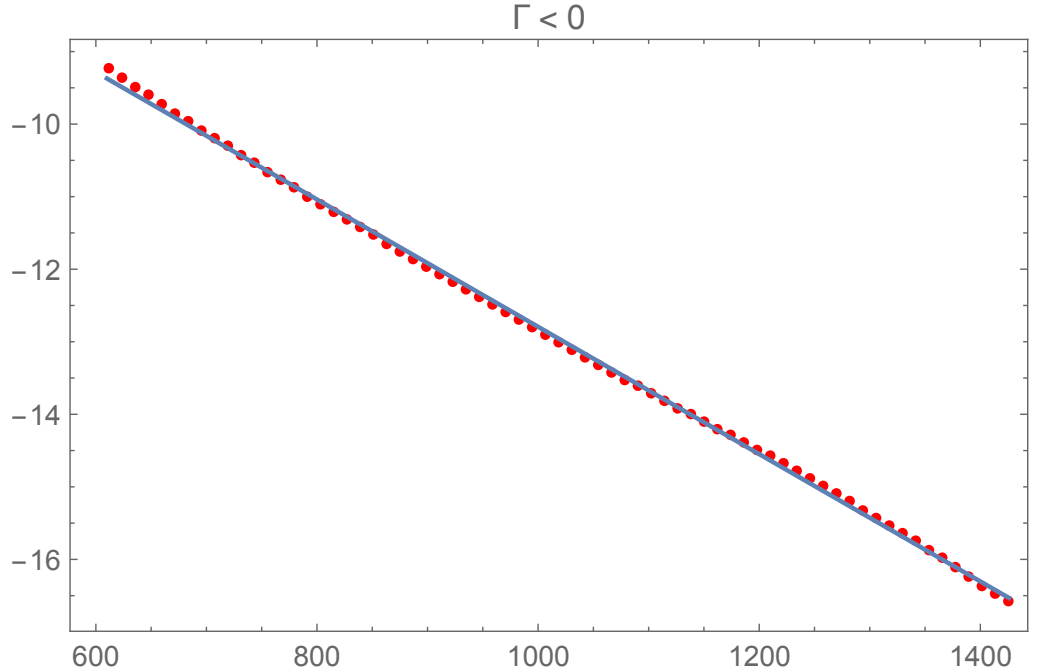


Figure 4. Fitting (102) for positive Γ .

The positive tail has the following fit in the inertial regime

	Estimate	Standard Error	t-Statistic	P-Value
A_+	-3.58916	0.0105971	-338.693	4.523×10^{-110}
B_+	-0.00925906	0.0000101328	-913.774	6.073×10^{-139}

Figure 5.

Figure 5. Fitting (102) for negative Γ .

The negative tail has the following fit in the inertial regime

	Estimate	Standard Error	t-Statistic	P-Value
A_-	-4.01871	0.0292907	-137.201	8.071×10^{-84}
B_-	-0.00877515	0.0000280073	-313.317	8.3194×10^{-108}

(105)

There is about 5% breaking of time-reversal symmetry $\Gamma \Rightarrow -\Gamma$ which is well beyond the statistical errors $\sim 10^{-3}$.

The ratio $\beta = \frac{B_-}{B_+} = 0.947737$.

Remarkably, one simple algebraic formula (93) for the loop wave function describes all the probability tails for velocity circulation, including the asymmetry of the left and right tails.²

It all follows from the Kelvinon solution of the Euler equation with a nontrivial winding number in an approximation of small relative fluctuations of the energy flow into a Kelvinon.

This approximation perfectly describes the tails of circulation PDF in DNS of strong isotropic turbulence.

4. Conclusions and Discussion

Now we can provide our answers to the questions posed in the Introduction.

- *What is the origin of the randomness of the circulating fluid?*

The origin of randomness is a large number of localized vortex blobs (Kelvinons) scattered far away from each other. These blobs contribute to the energy flow through the surface

² As for the low moments, they are mismatched in this solution. There is a regime change at some intermediate values of Reynolds number $\frac{\Gamma}{v}$. By construction, the Kelvinon solution only applies to intermittency phenomena. Our solution matched the Kelvinon asymptotic with DNS starting with $P < 10^{-7}$, $|\Gamma| > 610$.

around our isolated Kelvinon, creating random background velocity pointing in different directions.

Contributions of each blob to the background velocity decay as the third power of distance, but with a finite density of these blobs in infinite space, the random terms add up to finite Gaussian background velocity \vec{v}_0 .

The fluctuations of the energy flow in virtue of parity can be approximated as a quadratic form in background velocity. This dependence leads to our equilibrium distribution of the energy flow and, consequently, circulation.

- *Is it spontaneous, and what makes it irreversible?*

Yes, this randomness comes from inner vorticity distribution; in that sense, it is spontaneous. It does not need external forcing; it is self-consistent, like a mean field in the phase transition theory.

Ultimately, the energy comes from external forces at the boundary of the turbulent flow in an infinite volume. But the randomness influencing our isolated Kelvinon is the accumulated random background velocity contributing to the energy flux from other structures into this one. This random background velocity was measured in DNS and was shown to obey Gaussian distribution (see [8] [17] and references within).

Irreversibility (time-reflection breaking) comes from the Navier-Stokes anomalies. For arbitrary small viscosity, there is a finite contribution from the singular line of the Kelvinon vortex, regularized by a Burgers vortex at the core. In a limit, there are finite extra terms in the Euler Hamiltonian and the energy dissipation from singular vortexes.

The dissipation is linear with the tangent component of the strain along the loop; the sign of this variable changes at time reversal but is forced to be positive in the stable solution. Another source of spontaneous breaking of time reversal is the quantized circulation Γ_α of our Kelvinon. The winding number m is time-odd and can have two signs. A particular solution explicitly breaks this symmetry, leading to an asymmetric circulation PDF.

- *What are the properties of the fixed manifold covered by this random motion?*

This fixed manifold in our Kelvinon solution is a quadratic surface $\vec{v}_0 \cdot \hat{\Lambda} \cdot \vec{v}_0 = (\Gamma - \tau)\sigma, \vec{v}_0 \in R_3$ describing the velocity circulation Γ as a function of a vector of background velocity \vec{v}_0 .

Another way to describe this manifold is to consider the solution for the Clebsch field $\vec{S}(\vec{r}, \vec{v}_0)$. As a function of \vec{r} , it is a map $R_3 \mapsto S_2$, but this map also depends on a Gaussian random vector \vec{v}_0 covering the above quadratic surface.

On top of that, there is another degeneracy involved. The solution for \vec{S} is defined up to the symplectic transformation of coordinates in the target space, changing its metric while preserving the area and the topology. So, this solution represents a point on gauge orbit. There could be a time evolution around this orbit, corresponding to arbitrary time-dependent symplectic transformation, leaving invariant the velocity field.

- *Are there some "fundamental particles" hidden inside?*

This side remark by Feynman was a prophecy. He subconsciously reminded us about the fundamental particles, and he was right! There are confined quarks in turbulence, and they are called Faddeev variables or spherical Clebsch fields.

The vorticity and velocity are invariant under local symplectic transformations (44) of coordinates on the Clebsch target space. The sphere is a particular gauge choice in that gauge theory. Their topology is what makes the Kelvinon stable. There are remarkable "quantum" effects in classical turbulence related to the compactness of the classical motion of these fields in their target space S_2 .

One cannot observe spherical Clebsch as particle excitations, but one can study the structure of the vorticity field made from the Clebsch field³.

Why do we call these variables fundamental? They are canonical Hamiltonian variables with Poisson brackets of elementary rigid rotators or spins. All other variables (velocity, vorticity) are the gauge-invariant nonlinear functionals of these Clebsch fields.

5. New game for smart kids

Dear field theorists, topologists, and other advanced mathematical physicists! Stop looking at the end of the universe and inside the elementary particles – there is beauty and mystery right under your nose, in every river, every ocean, and even in the glass of wine, should you swirl it a little.

This work just scratched the surface of singular topological solutions in turbulence. The existence of Kelvinon as a minimum of a bounded Hamiltonian is plausible but not proven. There may be an exact solution, like an instanton in non-abelian gauge theory.

Dear numerical experimentalists! This theory can only be finished with your input, like any theory needing experimental data. There are so many predictions to verify besides the exponential decay of PDF. The spatial structure of the Kelvinon can be measured, and the predictions [11,12] for correlation functions on the discontinuity surface could be compared to more accurate numerical experiments.

Finally, the new breed of quantum computer enthusiasts! The loop equation is exact, and it describes a quantum system, which can be discretized and, after that, mapped directly to qubits. It could open the way to simulate extremely strong turbulence.

Acknowledgments

I greatly benefited from discussions of this theory since its early state with my friends and colleagues, especially Nikita Nekrasov, Sasha Polyakov, Pavel Wiegman, Grigory Volovik, Victor Yakhot, and Katepalli Sreenivasan. Their critical comments helped me fix errors, and their general skepticism inspired me to prove them wrong, not to mention their valuable positive contributions to this theory.

I am grateful to Joshua Feinberg and the participants of the Zoom colloquium at Haifa University for useful discussions.

Yang Hui-He, Thomas Fink, Arkady Tseytlin and other participants of my Lectures at the London Institute for Mathematical Sciences at the Royal Institution helped me formulate and understand the early version of this theory.

Deep discussions at the seminars in IAS were both inspiring and elucidating; I would like to thank Thomas Spenser, Sasha Polyakov, and other participants of the IAS seminars for their questions and comments.

I am especially grateful to Camillo De Lellis for his attention, questions, and critical comments while discussing this project. His deep insight into mathematical aspects of fluid dynamics and his rare ability to understand intuitive physics concepts were crucial for completing this work.

This research was partly supported by a Simons Foundation award ID 686282 at NYU Abu Dhabi. I am very grateful to Jim for his constant help and inspiration for my work, extending far beyond the financial support.

This project was completed while I was already working in ADIA. The atmosphere of creative freedom and academic research in the SPD department in ADIA, supported and encouraged by our Executive Director Majed Alromaithi, was essential in this final stage of my work. Thank you, Majed.

³ The thin vortex tubes of the type of the Burgers vortex were observed in DNS [22]

References

1. Migdal, A. Towards Field Theory of Turbulence, 2020, [\[arXiv:hep-th/2005.01231\]](https://arxiv.org/abs/hep-th/2005.01231).
2. Migdal, A. Probability Distribution of Velocity Circulation in Three Dimensional Turbulence, 2020, [\[arXiv:hep-th/2006.12008\]](https://arxiv.org/abs/hep-th/2006.12008).
3. Migdal, A. Clebsch confinement and instantons in turbulence. *International Journal of Modern Physics A* **2020**, *35*, 2030018, [\[arXiv:hep-th/2007.12468v7\]](https://arxiv.org/abs/hep-th/2007.12468v7). <https://doi.org/10.1142/s0217751x20300185>.
4. Migdal, A. Vortex sheet turbulence as solvable string theory. *International Journal of Modern Physics A* **2021**, *36*, 2150062, [\[https://doi.org/10.1142/S0217751X21500627\]](https://doi.org/10.1142/S0217751X21500627). <https://doi.org/10.1142/S0217751X21500627>.
5. Migdal, A. Confined Vortex Surface and Irreversibility. 1. Properties of Exact solution, 2021, [\[arXiv:physics.flu-dyn/2103.02065v10\]](https://arxiv.org/abs/physics.flu-dyn/2103.02065v10).
6. Migdal, A. Confined Vortex Surface and Irreversibility. 2. Hyperbolic Sheets and Turbulent statistics, 2021, [\[arXiv:physics.flu-dyn/2105.12719\]](https://arxiv.org/abs/physics.flu-dyn/2105.12719).
7. Migdal, A. Loop Equation and Area Law in Turbulence. In *Quantum Field Theory and String Theory*; Baulieu, L.; Dotsenko, V.; Kazakov, V.; Windey, P., Eds.; Springer US, 1995; pp. 193–231. <https://doi.org/10.1007/978-1-4615-1819-8>.
8. Iyer, K.P.; Sreenivasan, K.R.; Yeung, P.K. Circulation in High Reynolds Number Isotropic Turbulence is a Bifractal. *Phys. Rev. X* **2019**, *9*, 041006. <https://doi.org/10.1103/PhysRevX.9.041006>.
9. Wikipedia. Burgers vortex. https://en.wikipedia.org/wiki/Burgers_vortex, 2022. [Online; accessed 27-April-2022].
10. Migdal, A. Universal Area Law in Turbulence, 2019, [\[arXiv:1903.08613\]](https://arxiv.org/abs/1903.08613).
11. Migdal, A. Scaling Index $\alpha = \frac{1}{2}$ In Turbulent Area Law, 2019, [\[arXiv:1904.00900v2\]](https://arxiv.org/abs/1904.00900v2).
12. Migdal, A. Exact Area Law for Planar Loops in Turbulence in Two and Three Dimensions, 2019, [\[arXiv:1904.05245v2\]](https://arxiv.org/abs/1904.05245v2).
13. Migdal, A. Analytic and Numerical Study of Navier-Stokes Loop Equation in Turbulence, 2019, [\[arXiv:1908.01422v1\]](https://arxiv.org/abs/1908.01422v1).
14. Migdal, A. Loop equations and $\frac{1}{N}$ expansion. *Physics Reports* **1983**, *201*.
15. Kuznetsov, E.; Mikhailov, A. On the topological meaning of canonical Clebsch variables. *Physics Letters A* **1980**, *77*, 37–38. [https://doi.org/10.1016/0375-9601\(80\)90627-1](https://doi.org/10.1016/0375-9601(80)90627-1).
16. Levich, E. The Hamiltonian formulation of the Euler equation and subsequent constraints on the properties of randomly stirred fluids. *Physics Letters A* **1981**, *86*, 165–168.
17. Iyer, K.P.; Bharadwaj, S.S.; Sreenivasan, K.R. The area rule for circulation in three-dimensional turbulence. *Proceedings of the National Academy of Sciences of the United States of America* **2021**, *118*, e2114679118. <https://doi.org/10.1073/pnas.2114679118>.
18. Sreenivasan, K.R.; Yakhot, V. Dynamics of three-dimensional turbulence from Navier-Stokes equations. *Phys. Rev. Fluids* **2021**, *6*, 104604. <https://doi.org/10.1103/PhysRevFluids.6.104604>.
19. Sreenivasan, K.R.; Yakhot, V. The saturation of exponents and the asymptotic fourth state of turbulence, 2022. <https://doi.org/10.48550/ARXIV.2208.09561>.
20. Gurarie, V.; Migdal, A. Instantons in the Burgers equation. *Phys. Rev. E* **1996**, *54*, 4908–4914. <https://doi.org/10.1103/PhysRevE.54.4908>.
21. Polyakov, A.M. Turbulence without pressure. *Physical Review E* **1995**, *52*, 6183–6188. <https://doi.org/10.1103/physreve.52.6183>.
22. Buaria, D.; Pumir, A.; Bodenschatz, E.; Yeung, P.K. Extreme velocity gradients in turbulent flows. *New Journal of Physics* **2019**, *21*, 043004. <https://doi.org/10.1088/1367-2630/ab0756>.

Appendix A Initial data for the Kelvinon

Let us present an explicit example of the Clebsch field with required topology, which could serve as initial data for the Hamiltonian minimization by relaxation.

We introduce a surface of the minimal area bounded by our loop C

$$S_{min}(C) = \arg \min_{S: \partial S = C} \int_S dS \quad (A106)$$

For every point $\vec{r} \in R_3$, there is the nearest point \vec{r}_1 at the minimal surface $\mathcal{S}_{min}(C)$.

$$\vec{r}_1 = \arg \min_{\vec{r}' \in \mathcal{S}_{min}(C)} (\vec{r} - \vec{r}')^2; \quad (\text{A107})$$

For this point \vec{r}_1 at the surface there is also a nearest point \vec{r}_0 at its edge C , minimizing the geodesic distance $d(a, b)$ along the surface from \vec{r}_1 to the edge

$$s_0 = \arg \min_s d(\vec{r}_1, \vec{C}(s)); \quad (\text{A108})$$

$$\vec{r}_0 = \vec{C}(s_0); \quad (\text{A109})$$

Let us also introduce the local frame with vectors $\vec{t}(s), \vec{n}(s), \vec{\sigma}(s)$ at the loop:

$$\vec{C}'(s)^2 = 1; \quad (\text{A110a})$$

$$\vec{t}(s) = \vec{C}'(s); \quad (\text{A110b})$$

$$\vec{n}(s) = \frac{\vec{C}''(s)}{|\vec{C}''(s)|} \quad (\text{A110c})$$

$$\vec{\sigma}(s) = \vec{t}(s) \times \vec{n}(s); \quad (\text{A110d})$$

Our field is then defined as follows:

$$\alpha = \frac{2\pi s_0}{\oint |d\vec{C}|}; \quad (\text{A111a})$$

$$\beta = \arg((\vec{r} - \vec{r}_0) \cdot (\vec{n}(s_0) + i\vec{\sigma}(s_0))); \quad (\text{A111b})$$

$$\rho = \sqrt{(\vec{r} - \vec{r}_1)^2 + d(\vec{r}_1, \vec{r}_0)^2}; \quad (\text{A111c})$$

$$S_1 + iS_2 = \frac{2\lambda\rho}{\lambda^2 + \rho^2} e^{im\alpha + i(n+\frac{1}{2})\beta}; \quad (\text{A111d})$$

$$S_3 = \frac{\lambda^2 - \rho^2}{\lambda^2 + \rho^2}; \quad (\text{A111e})$$

The parameter λ plays the role of the size of the Kelvinon in physical space R_3 .

When the point \vec{r} approaches the nearest point \vec{r}_1 at the minimal surface, the difference $\vec{r} - \vec{r}_1$ is normal to this surface.

When the point \vec{r}_1 approaches the nearest point \vec{r}_0 at the edge C of the surface, the geodesic becomes a straight line in R_3 , tangent to the surface and ρ becomes Euclidean distance to the loop

$$d(\vec{r}_1, \vec{r}_0) \rightarrow |\vec{r}_1 - \vec{r}_0|; \quad (\text{A112})$$

$$\rho^2 \rightarrow |\vec{r} - \vec{r}_1|^2 + |\vec{r}_1 - \vec{r}_0|^2 = |\vec{r} - \vec{r}_0|^2 \quad (\text{A113})$$

Note that all variables $s_0, \vec{r}_0, \vec{r}_1, \alpha, \beta, \rho, \vec{S}$ depend on $\vec{r} \in R_3$ through the minimization of the distance to the surface and the loop. By construction, $\rho = |\vec{r} - \vec{r}_0|$ away from the surface, when $\vec{r}_1 = \vec{r}_0, d(\vec{r}_1, \vec{r}_0) = 0$.

The Clebsch field $\vec{S}(\vec{r})$ takes the boundary value $\vec{S}(C) = (0, 0, 1)$ at the loop and $\vec{S}(\infty) = (0, 0, -1)$.

One may estimate the decay rate of $\vec{\nabla}S_3 \sim 1/|\vec{r}|^3, \vec{\nabla}\phi_2 \sim 1/|\vec{r}|$, which corresponds to vorticity decaying as $1/|\vec{r}|^4$.

This decay is sufficient for the convergence of the enstrophy integral at infinity.

Let us move \vec{r} along the normal from the surface at \vec{r}_1 . Our parametrization of S_3 does not change in the first order in normal shift $\vec{\eta} = \vec{r} - \vec{r}_1$, as ρ^2 has only quadratic terms in $\vec{\eta}$.

We conclude that the normal derivative of the Clebsch field $\phi_1 = Z(1 + S_3)$ vanishes

$$\partial_n \phi_1 = 0; \quad (\text{A114})$$

We requested vanishing normal velocity at the discontinuity surface for this surface to be stationary. In terms of Clebsch parametrization (55) the normal velocity would vanish provided

$$\partial_n \Phi = \left(\vec{\nabla} \times \Psi \right)_n; \quad \vec{r} \in S_C / \mathcal{T} \quad (\text{A115})$$

As for the angular field $\phi_2 = \phi$ in (A111), its normal derivative does not vanish in the general case. The angle α does not change when the point \vec{r} moves in normal direction $\vec{N}(\vec{r}_1)$ from the surface projection \vec{r}_1 by infinitesimal shift $\vec{\eta} = \epsilon \vec{N}(\vec{r}_1)$. However, another angle β changes in the linear order in ϵ as

$$\vec{N}(\vec{r}_1) \cdot (\vec{n}(s_0) + \iota \vec{\sigma}(s_0)) \neq 0 \quad (\text{A116})$$